Arabian Journal of Chemistry (2021) **14**, 102953

King Saud University

Arabian Journal of Chemistry

www.ksu.edu.sa
www.sciencedirect.com

ORIGINAL ARTICLE

Effect of potassium permanganate on morphological, structural and electro-optical properties of graphene oxide thin films

Muhammad Kashif [a,*], Erdawaty Jaafar [b], Poonam Bhadja [c,d,*], Foo Wah Low [e], Siti Kudnie Sahari [f], Shahid Hussain [g], Foo Kai Loong [h], Awais Ahmad [i], Tahani Saad AlGarni [j], Muhammad Shafa [k], Humaira Asghar [l], Saad A. Al-Tamrah [j]

[a] *School of Electrical & Information Engineering, Tianjin University, 92 Weijin Road, Nankai District, Tianjin 300072, China*
[b] *LTI Engineering, Project Department, Puchong Business Park 47160, Puchong, Selangor, Malaysia*
[c] *Arthropod Ecology and Biological Control Research Group, Ton Duc Thang University, Ho Chi Minh City, Viet Nam*
[d] *Faculty of Environment and Labour Safety, Ton Duc Thang University, Ho Chi Minh City, Viet Nam*
[e] *Department of Electrical & Electronic Engineering, Lee Kong Chian, Faculty of Engineering & Science, Universiti Tunku Abdul Rahman, Bandar Sungai Long, 43000 Kajang, Selangor, Malaysia*
[f] *Faculty of Engineering, Universiti Malaysia Sarawak, 94300 Kota Samarahan, Sarawak, Malaysia*
[g] *School of Materials Science and Engineering, Jiangsu University, Zhenjiang 212013, China*
[h] *Institute of Nano Electronic Engineering, Universiti Malaysia Perlis, Malaysia*
[i] *Department of Chemistry, The University of Lahore, Lahore 54590, Pakistan*
[j] *Department of Chemistry, College of Science, King Saud University, Riyadh 11451, Saudi Arabia*
[k] *State Key Laboratory for Mechanical Behavior of Materials, School of Materials Science and Engineering, Xi'an Jiaotong University, Xi'an 710049, China*
[l] *Department of Chemistry, Government College University Faisalabad, 38000, Pakistan*

Received 17 October 2020; accepted 13 December 2020
Available online 22 December 2020

KEYWORDS

Potassium permanganate;
Graphene oxide;
Oxidizing agent;
Thin film;

Abstract This work investigated the effect of Potassium Permanganate ($KMnO_4$) on graphene oxide (GO) properties, especially on electrical properties. The GO thin films were deposited on a glass substrate using drop casting technique and were analysed by using various type of spectroscopy (e.g. Scanning Electron Microscopy (SEM), Ultra- Violet Visible (UV–VIS), Fourier Transform Infrared (FTIR), X-Ray Diffraction (XRD), optical band gap, Raman Spectroscopy).

* Corresponding authors at: School of Electrical & Information Engineering, Tianjin University, 92 Weijin Road, Nankai District, Tianjin 300072, China (Muhammad Kashif). Arthropod Ecology and Biological Control Research Group, Ton Duc Thang University, Ho Chi Minh City, Viet Nam (Poonam Bhadja).
E-mail addresses: mkashif@tju.edu.cn (M. Kashif), poonam.bhadja@tdtu.edu.vn (P. Bhadja).
Peer review under responsibility of King Saud University.

Production and hosting by Elsevier

https://doi.org/10.1016/j.arabjc.2020.102953

Electrical

Furthermore, the electrical experiments were carried out by using current–voltage (*I-V*) characteristic. The GO thin film with 4.5 g of $KMnO_4$ resulted in higher conductivity which is 3.11×10^{-4} S/cm while GO with 2.5 g and 3.5 g of $KMnO_4$ achieve 2.47×10^{-9} S/cm and 1.07×10^{-7} S/cm, respectively. This further affects the morphological (SEM), optical (band gap, UV–Vis, FTIR, and Raman), and crystalline structural (XRD) properties of the GO thin films. The morphological, elemental, optical, and structural data confirmed that the properties of GO is affected by different amount of $KMnO_4$ oxidizing agent, which revealed that GO can potentially be implemented for electrical and electronic devices.

1. Introduction

Nowadays, carbonaceous nanomaterial have undergone an enormous interest owing to their unique combination of physicochemical properties (Qu et al., 2018). Among the family of carbonaceous, GO consists of a two dimensional network of sp^2 and sp^3 linked atoms, as opposed to an ideal graphene sheet consisting of 100% sp^2 hybridized carbon atoms (Soldano et al., 2010). For more than a century, GO has been known as a graphite exfoliation yield (Brodie, 1859; Hummers and Offeman, 1958) through the reaction of graphite powders with strong oxidizing agent such as potassium permanganate ($KMnO_4$) in concentrated sulphuric acid (Brodie, 1859; Panicker et al., 2020). Several oxygenated functional group was decorated in atomic sheet of graphite on its basal plane and its edges known as GO, resulting in a hybrid structure comprising a composite of sp^2 and sp^3 hybridized carbon atoms (Geim and Novoselov, 2007). The sp^2/sp^3 ratios of the carbon atoms can be altered by tuning the degree of oxidation and in turn, it will affect the properties of GO (Jeong et al., 2010). The formation of sp^3 domain is generated by the oxidation reaction which results in the diverse types of termination groups such as –OH, epoxy, -COR' and –COOH groups (Cai et al., 2008; Jung et al., 2009). The presence of these oxygenated functional groups allow GO to become hydrophilic and later enable them to function with other materials with suitable chemistry (Veerapandian et al., 2012). Graphene oxide (GO) has numerous applications in high-speed semiconductors (Murakami et al., 2019), flexible devices (Budimir et al., 2019; Yang et al., 2020), optoelectronics (Marrani et al., 2019; Pargoletti et al., 2020), and energy storage (Thota, Wang et al., 2021; Zhang et al., 2019; Zhou et al., 2020).

This paper reports on the synthesis of GO by varying the amount of $KMnO_4$. It is a fact that GO synthesis is highly correlated with its properties and the nature of its groups is strongly reliant upon the oxidation level of GO. In view of this, this study is to investigate the properties of GO by varying spectroscopic techniques and, *I-V* characteristics.

2. Experimental method

2.1. Materials

The raw graphite flakes was purchased from Sigma Aldrich (USA). The $KMnO_4$ was supplied by R&M Chemicals. The hydrochloric (HCl) and sulphuric (H_2SO_4) acids were obtained from Fisher Scientific. The phosphoric acid (H_3PO_4) and hydrogen peroxide (H_2O_2) were bought from Macron Chemicals and Merck. All these chemicals were analytical reagents (AR) grades.

2.2. Designation of prepared GO

Comprehensively, three samples of GO were prepared using the equal quantity of graphite powder, reaction temperature, and time parameter. Nevertheless, the amount of $KMnO_4$ with vary in 2.5 g, 3.5 g and 4.5 g are being prepared for the GO samples for oxidation level investigation study, which are labelled as GOA, GOB, and GOC, respectively,

2.3. Synthesis of GO

The synthesis of GO via Improved Hummer's method has been reported in our previous work (Low et al., 2017). GO was formulated by the oxidation of natural graphite powder using the adaptive approach. In brief, 0.75 g of graphite powder was introduced to $KMnO_4$ with different masses (2.5 g, 3.5 g and 4.5 g). Then, the resultant mixture of H_2SO_4:H_3PO_4 in the ratio of 90 ml:10 ml was introduced slowly. Eqs. (1) and (2) took place in the reaction between $KMnO_4$ and H_2SO_4 which produced diamanganese heptoxide (Mn_2O_7) that is used to oxidize the graphite (Shamaila et al., 2016).

$$KMnO_4 + 3H_2SO_4 \rightarrow K^+ + MnO_3^+ + H_3O^+ + 3HSO_4^- \quad (1)$$

$$MnO_3^+ + MnO_4^- \rightarrow Mn_2O_7 \quad (2)$$

The temperature of reaction was kept at 50 °C and under continuous stirring for 48 h. The mixture color was adjusted its self from dark purplish green to dark purple and light purple depending on the mass of $KMnO_4$. Then reaction mixture was kept cold to room temperature and dumped into an ice filled beaker around 20 °C. The mixture was quenched with 0.75 ml of H_2O_2 at room temperature to form dark yellow suspension GO. The cleaning cycle was carried out using simple decantation of precipitate through centrifugation technique at 6000 rpm for 10 mins. The suspension was washed repeatedly with HCl (three times) and deionized water (two times) which led to GO formation around pH10. Afterwards, it was cured at 60 °C for 10 min. Subsequently, 10 mg of GO powder was dissolved in 5 ml of distilled water and sonicated until no visible particle detectable. Each of the glass substrates were ultrasonically washed in acetone, isopropanol, ethanol and lastly distilled water for 10 min. The substrates were dried with the blow of hot air. Then GO solution was deposited on glass by drop casting method and dried for 10 min at 60 °C.

2.4. Preparation of GO thin film

For GO thin film deposition, a 30 mg of GO powder was dispersed in 5 ml of distilled water and was sonicated until no visible particle can be seen. The glass substrates were ultrasonically cleaned in acetone, isopropanol, ethanol and distilled water for 10 min, respectively. After that, the glass substrates were dried using an air blow. Drop casting method was used for deposition of GO solution on a glass substrate. The deposited solution was dried 60 °C for 10 min under ambient condition. In order to measure the electrical properties, a showdown mask was used to deposit gold electrodes on top of as deposited films by using sputter coater having length and width of 1 cm and 1.5 cm, respectively. Whereas the distance between the electrodes were maintained at 1 cm. Keithley 2450 source-meter was used to measure the electrical properties of as prepared form.

2.5. Characterization

The UV–Visible spectroscopy (1800 Shimadzu) was used to detect the absorption of GO in the range of 200 nm to 800 nm. The characterization continued with Fourier Transform Infrared (Shimadzu IRAffinity-1). The spectral recorded ranges from 1400 cm^{-1} to 1700 cm^{-1} with a resolution of 2 cm^{-1} and 4 cm^{-1} average. The morphological structure of GO was observed through scanning electron microscopy (TM3030 Hitachi). X-Ray Diffraction (PANalytical X'PERT PRO MRD PW 3040/60) was employed to detect the presence of the phases. Horiba Jobin Yvon HR 800 UV Raman was engaged to detect the wavelength spectrum with 514 nm. Electrical properties were carried out using Keithley 2450 source-meter.

3. Results and discussion

3.1. Visual characteristic

Optical observation is a direct way to monitor the differences that was caused by the effects of different amount of $KMnO_4$ on GO. The difference in the amounts of $KMnO_4$ could improve the electrical conductivity and properties of GO either in morphological, optical and structural properties. Indeed, the effect of oxidation reaction studies were verified through these three different synthesized GO powder in the variation of $KMnO_4$ amount that denoted as GOA, GOB and GOC. Fig. 1 shows the visible examination of all the samples, and it can be observed that the color changes from blackish to brownish yellow due to the levels of oxygenated functional groups (Veerapandian et al., 2012).

3.2. Morphological properties

Fig. 2 displays the SEM images of GO at different amount of $KMnO_4$ from 2.5 g to 4.5 g. The absence of the crumpled structure that could be observed in Fig. 2(a) reveals that the graphite is not fully oxidized due to inadequate oxidizing agent. In fact, the formation of GO can be produced from the exfoliation of graphite by introducing strong oxidizing agent (Compton et al., 2012). Fig. 2(b) exhibits the crumpled

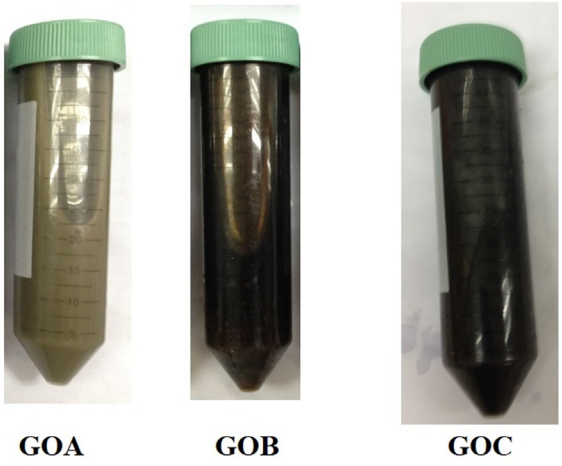

Fig. 1 Photographic images of GO samples with different amount of $KMnO_4$.

structure which indicates the starting exfoliation process of graphite. The existing crumpled and rippled structure shown in Fig. 2(c) indicated that the graphite is fully exfoliated due to deformation during the exfoliation and restacking process which is in good agreement with reported literature (Alazmi et al., 2016). Table 1 briefly summarized for the content of C and O elements that mainly occupied for these three samples. The percentage of C is gradually decreased while increased in the terms of O element. The results were attributed to the optimum of 4.5 g sufficient react in the GOC sample to form specific essential oxygenated groups.

3.3. Structural properties

XRD analysis is used to describe the crystalline structure and phase purity of the synthesized GO at different amount of $KMnO_4$. For 2.5 g of $KMNO_4$, there was no significant peaks appeared before 20°, as could be observed in Fig. 3(a), credited to the incomplete oxidation of graphite. After that, a broad band attended around 15–35°, which demonstrated an amorphous and/or a nano-crystalline structure for the prepared glass and ITO thin films, corresponds to the well-arranged carbon structure layer along (002) orientation (Davood and Faegh, 2012). In contrast, Fig. 3(b–c) shows that there have an insignificant diffraction peak appeared at 10.63°. It corresponded with an interlayer spacing of about 0.83 nm which is close to the reported literature (Emiru and Ayele, 2017). In addition, it also shows that the exfoliation of graphite had occurred and consequently proves that the exfoliation of graphite is dependent on the oxidation level of GO.

3.4. Optical properties

3.4.1. Fourier transform infrared (FTIR)

As shown in Fig. 4(a–c), FTIR spectroscopy was used to classify the identity of oxygenated functional groups in GO. The spectrum in Fig. 4(a) shows a broad absorption band at 1641 cm^{-1} due to the presence C═C bond in graphitic domain (Veerapandian et al., 2012). Furthermore, the presence of more oxygen functional groups in Fig. 4(b) where the O—H bond is

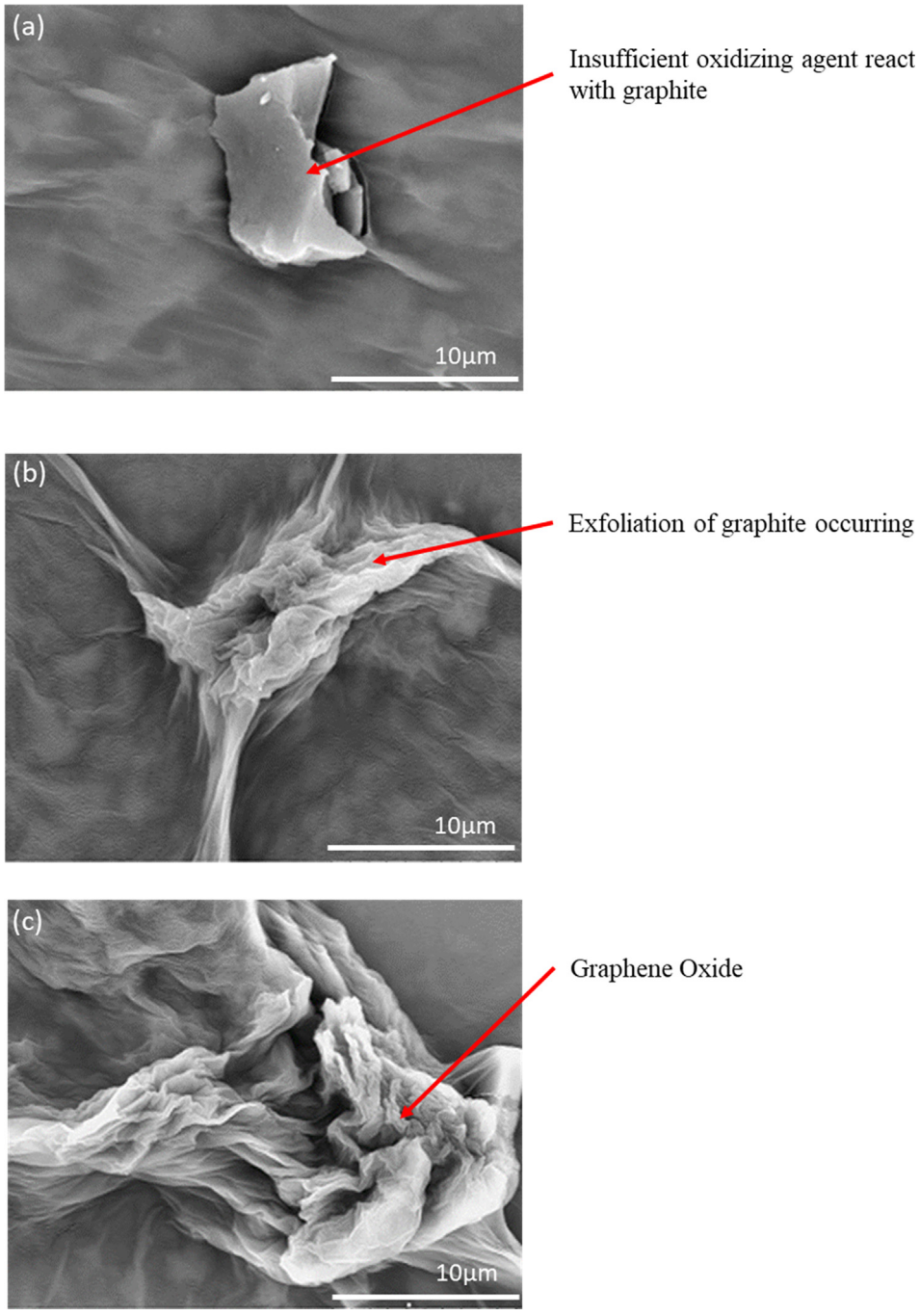

Fig. 2 SEM images of (a) GOA (b) GOB (c) GOC.

Table 1 EDX Results of GOA, GOB, and GOC.

Samples	Carbon, C (at.%)	Oxygen, O (at.%)	Total (at.%)
GOA	83.29	16.71	100.00
GOB	71.03	28.97	100.00
GOC	66.47	33.53	100.00

at 1415 cm^{-1} due to the increasing oxidation level of graphite. More functional groups are present with the increasing of oxidation level. This can be observed in Fig. 4(c). A broad and intense band appeared along 3400 cm^{-1} was attributed to hydroxyl group (–OH) for GOA, GOB, and GOC, respectively. Accordingly, minor peak of –OH functional group at 3750 cm^{-1} was also determined that oxygen molecules

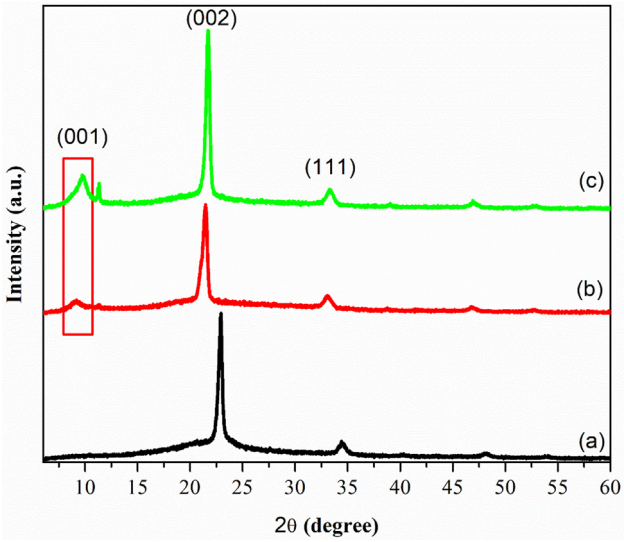

Fig. 3 XRD pattern of a) GOA b) GOB c) GOC.

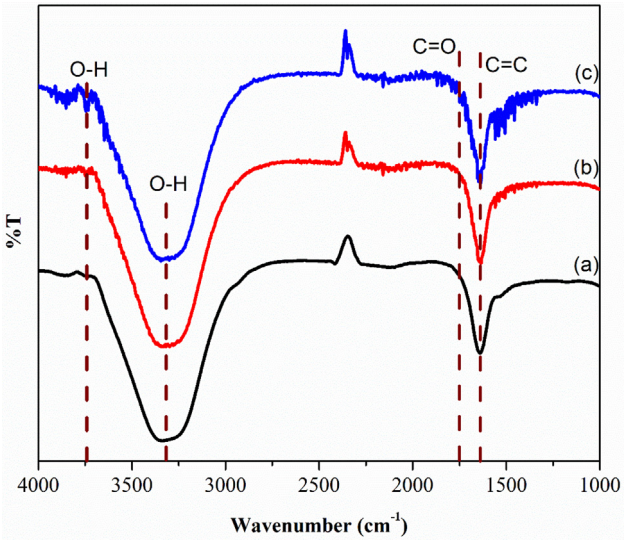

Fig. 4 FTIR of (a) GOA (b) GOB (c) GOC.

attended during oxidation process and fully oxidized from graphite.

3.4.2. Raman spectroscopy

Raman spectroscopy gave an instant structural information and quality characterization of GO thin films. Fig. 5(a–c) dictates that the intensity of the G-band symmetry was higher compared to the D-band symmetry. This is due to the vibration of sp^2 bonded of carbon atoms (Krishnamoorthy et al., 2012) and the wavenumber of the G-band that is closer to 1580 cm^{-1} (Ferrari et al., 2006). As reported in the previous work (Wang et al., 2011), the G-band peak (1580 cm^{-1}) refers to the symmetry of carbon atoms while the D-band peak (1350 cm^{-1}) corresponds to the disorder induction of carbon atoms (Venugopal et al., 2011). Fig. 5 (a) shows the shift of G band towards a higher wave number at 1580 cm^{-1}, which owing to the graphite oxidation. Meanwhile, the D band has

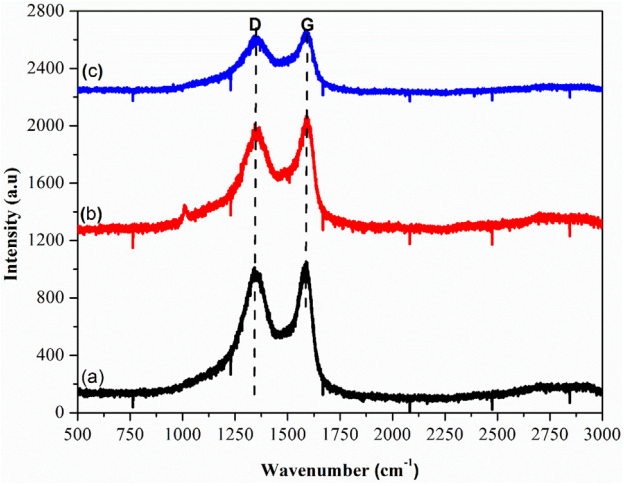

Fig. 5 Raman Spectra of (a) GOA (b) GOB (c) GOC.

an intense amplitude, which can be due to the formation of defects and disorder such as the presence of in plane hetero atoms, grain boundaries, and aliphatic chain (Pimenta et al., 2007). The shift of G band peaks (1595 cm^{-1} and 1600 cm^{-1}) were also observed in Fig. 5(b–c) which indicates the oxidation level of graphite. Thus, the occurrence of graphite exfoliation depends on the oxidation level that was caused by the oxidizing agent ($KMnO_4$). In addition, the sp^3 domain also increases with the rise of oxidation level due to the disruption of graphitic stacking order (Muzyka et al., 2017).

GOA, GOB and GOC records I_D/I_G ratio of 0.96, 0.91 and 0.90, respectively. It also shows that lower oxidation levels resulted in an increase in the I_D/I_G ratio, which in turn decreases with the increase of oxidation. Moreover, the occurrence of sp^2 hybridized carbon was relative to the intensities of the D and G-band (I_D/I_G) in the degree of symmetry or defects (Novoselov et al., 2004).

3.4.3. Ultraviolet–visible spectroscopy (UV–Vis)

Fig. 6 shows the optical properties of deposited GO thin films at different amount of $KMnO_4$. Fig. 6 (a) revealed that the maximum absorption peak was at 231 nm whereas Fig. 6 (b-c) shifted to lower wavelength probably due to the decrease of delocalized electron (He and Fang, 2016; Mei et al., 2010). In addition, these peak corresponded to π to π^* transition for the C═C bonding (Mei et al., 2010). A similar shoulder was also observed around 300 nm for all three samples which is attributed to n to π^* transition of the carbonyl groups (C═O) (Marcano et al., 2010). The enhanced absorbance was observed in Fig. 6(a–c) and it can be concluded that the intensity of GO peaks increases along with the increased amount of $KMnO_4$ from 2.5 g to 4.5 g. This suggests that an adequate amount of oxidizing agent is required for graphite exfoliation (He and Fang, 2016). Thus the absorption band around 300 nm indicated the degree of oxidation (Emiru and Ayele, 2017).

The optical band gap of GO with various amount of $KMnO_4$ is exhibited in Fig. 7. It is generated from Fig. 6 by using typical Planck calculation. The Tauc plot shown the values of optical band gap energy gradually decrease from 4.46 eV

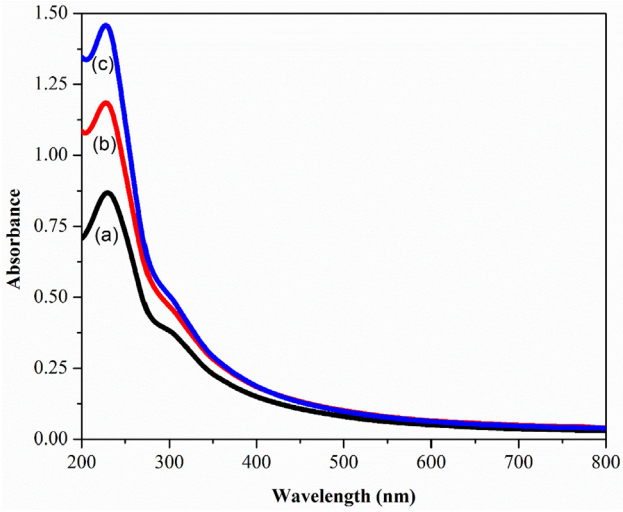

Fig. 6 UV–Vis Spectroscopy of a) GOA b) GOB c) GOC.

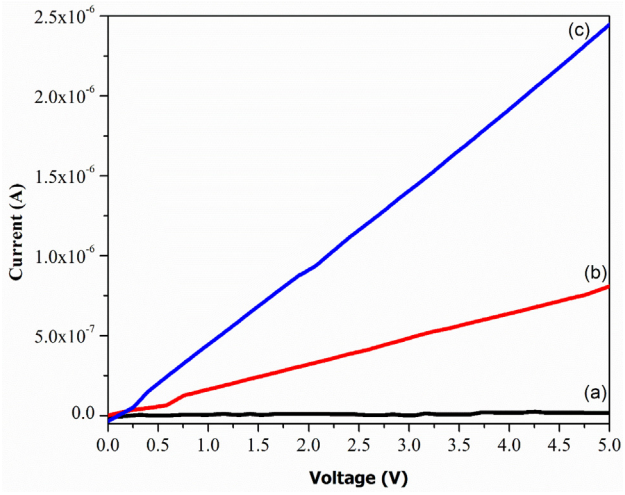

Fig. 8 *I-V* Characteristic of a) GOA b) GOB c) GOC.

to 4.35 eV as increase in amount of $KMnO_4$ (Manoj et al., 2017; Yahia and Mohammed, 2018). The changing of optical band gap with respect to amount of $KMnO_4$ can be attributed to the exfoliation of graphite (Wang et al., 2013).

3.5. Electrical properties

Fig. 8 exhibits electrical properties of the deposited GO thin films with different amount of $KMnO_4$. There is an increment in current values as shownin Fig. 8(a–c) which is from 1.08×10^{-8} to 1.36×10^{-6} A. Beside the resistivity is significantly decreases from 9.33×10^{6} Ω.cm (GOB) to 3.21×10^{3} Ω.cm (GOC). The rationale behind this was due to the exfoliation of graphite caused by the presence of more oxygen functional groups (Veerapandian et al., 2012). A smaller current value was observed in Fig. 8(a) which was due to deficient oxidation level of GO. Therefore, it is evident that the electrical properties of GO are highly dependent on the oxygen contents

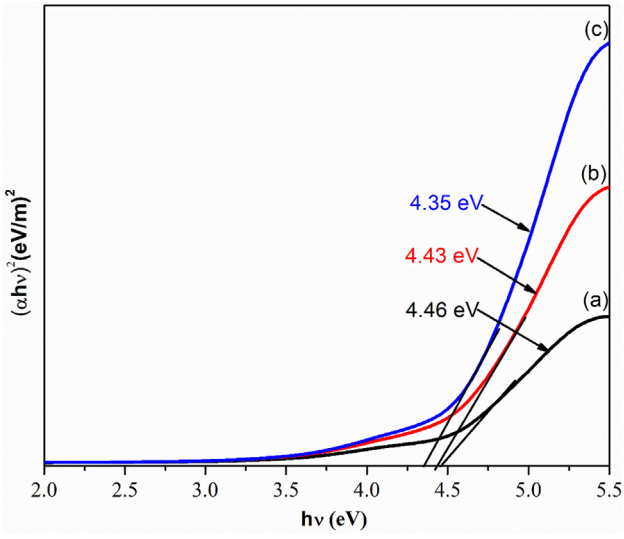

Fig. 7 Optical Band Gap of a) GOA b) GOB c) GOC.

which is supported by Guerrero-Contreras and Caballero-Briones (2015). Hoffman reported that good GO is obtained from the oxidation of graphite with strong oxidizing agents (Bonaccorso et al., 2012). Table 2 is generated from Fig. 8 by using typical *I-V* calculation. The overall conductivity increases with the increasing of oxidation level due to exfoliation of graphite (Low et al., 2020a). Besides, the resistivity also dramatically increased while the content of $KMnO_4$ increases due to the oxygenated functional groups is more active with well-formed of bonding at the edge of exfoliated graphene oxide layer (Epoxy group, hydroxyl group, carboxyl group, and etc.) (Eda et al., 2013; Low et al., 2020b; Skákalová et al., 2018). This phenomenon is made a strong agreement with Fig. 4. Indeed, the decreased of I_D/I_G ratio might indicated that multilayer of GO is formed and also contributed by the distortion (lattice) defects (Low, Lai, and Abd Hamid, 2015). Henceforth, this work shows a significant improvement in the electrical properties of GO which is better than that of reported prior to this study (Guerrero-Contreras and Caballero-Briones, 2015; Venugopal et al., 2012).

4. Conclusion

The improved technique was successfully employed in the preparation of GO with various amount of oxidizing agent, $KMnO_4$. The effect of oxidation level on properties of GO were intensively investigated in aspect of morphology, functional groups, optical, crystallinity, and GO structure/bonding within molecules. There were produced almost similar in terms of functional groups although synthesized in the variety of different mass $KMnO_4$. Furthermore, 4.5 g performed in the lowest energy band gap due to the fully exfoliated and established a stable GO layer with highly crystalline and could enhance the electrical properties greatly. On the other hands, the attendance of peak in XRD could further determined that well-aligned of carbon structure in the arrangement of D-spacing along (002) orientation. At last but not least, the obtained I_D/I_G ratio gradually decreased clearly determined that the 4.5 g $KMnO_4$ is the optimum oxidizing agent amount due to the well-formed of sp^2-hybridized carbon with good bonding of exfoliated GO sample. For future prospects, the oxidation

Table 2 Effects of electrical and optical properties of GO at different masses of KMnO4.

SampleLabel	Resistance,Ω	Resistivity, [Ω.cm]	Conductivity, [S/cm]	I_D/I_G Ratio	Eg (*eV*)
GOA	270×10^6	405×10^6	2.47×10^{-9}	0.96	4.46
GOB	6.22×10^6	933×10^6	1.07×10^{-7}	0.91	4.43
GOC	2.14×10^6	3.21×10^3	3.11×10^{-4}	0.90	4.35

level of GO can potentially be applied for electrical and electronic applications as well as photovoltaic cell to enhance its overall efficiency and performance.

CRediT authorship contribution statement

Muhammad Kashif: Supervision, Writing - review & editing, Investigation. **Erdawaty Jaafar:** Writing - original draft, Investigation, Methodology. **Poonam Bhadja:** Conceptualization, Writing - review & editing. **Foo Wah Low:** Writing - review & editing. **Siti Kudnie Sahari:** Formal analysis. **Shahid Hussain:** Conceptualization. **Foo Kai Loong:** Formal analysis. **Awais Ahmad:** Formal analysis. **Tahani Saad AlGarni:** Funding acquisition, Writing - review & editing. **Muhammad Shafa:** Formal analysis. **Humaira Asghar:** Review & editing. **Saad A. Al-Tamrah:** Review & editing.

Declaration of Competing Interest

The authors declare that they have no known competing financial interests or personal relationships that could have appeared to influence the work reported in this paper.

Acknowledgments

The authors would like to thank all colleagues and technicians from the Faculty of Engineering and Faculty of Resource Science & Technology, University Malaysia Sarawak (UNIMAS) for the assistance and technical support, encouragement, and guidance throughout this work Dr. Tahani Saad AlGarni is grateful to Researchers Supporting Project number (RSP-2020/254), King Saud University, Riyadh, Saudi Arabia, for financial assistance.

Funding Statement

This project is granted by the Ministry of Higher Education Malaysia (MOHE) via Fundamental Research Grant Scheme FRGS/SG06 (02)/1287/2015(04), start-up fund from Tianjin University, China and Researchers Supporting Project number (RSP-2020/254), King Saud University, Riyadh, Saudi Arabia.

References

Alazmi, A., Rasul, S., Patole, S.P., Costa, P.M.F.J., 2016. Comparative study of synthesis and reduction methods for graphene oxide. Polyhedron 116, 153–161. https://doi.org/10.1016/j.poly.2016.04.044.

Bonaccorso, F., Lombardo, A., Hasan, T., Sun, Z., Colombo, L., Ferrari, A.C., 2012. Production and processing of graphene and 2d crystals. Mater. Today 15 (12), 564–589. https://doi.org/10.1016/S1369-7021(13)70014-2.

Brodie, B.C., 1859. XIII. On the atomic weight of graphite. Philos. Trans. R. Soc. Lond. 149, 249–259. https://doi.org/10.1098/rstl.1859.0013.

Budimir, M., Jijie, R., Ye, R., Barras, A., Melinte, S., Silhanek, A., Boukherroub, R., 2019. Efficient capture and photothermal ablation of planktonic bacteria and biofilms using reduced graphene oxide-polyethyleneimine flexible nanoheaters. J. Mater. Chem. B 7 (17), 2771–2781. https://doi.org/10.1039/c8tb01676c.

Cai, W., Piner, R.D., Stadermann, F.J., Park, S., Shaibat, M.A., Ishii, Y., Ruoff, R.S., 2008. Synthesis and solid-state NMR structural characterization of < sup > 13 < /sup > C-labeled graphite oxide. Science 321 (5897), 1815–1817. https://doi.org/10.1126/science.1162369.

Compton, O.C., Cranford, S.W., Putz, K.W., An, Z., Brinson, L.C., Buehler, M.J., Nguyen, S.T., 2012. Tuning the mechanical properties of graphene oxide paper and its associated polymer nanocomposites by controlling cooperative intersheet hydrogen bonding. ACS Nano 6 (3), 2008–2019. https://doi.org/10.1021/nn202928w.

Davood, R., Faegh, H., 2012. Surface morphology dynamics in ITO thin films. J. Modern Phys. 2012.

Eda, G., Nathan, A., Wöbkenberg, P., Colleaux, F., Ghaffarzadeh, K., Anthopoulos, T.D., Chhowalla, M., 2013. Graphene oxide gate dielectric for graphene-based monolithic field effect transistors. Appl. Phys. Lett. 102, (13) 133108.

Emiru, T.F., Ayele, D.W., 2017. Controlled synthesis, characterization and reduction of graphene oxide: a convenient method for large scale production. Egypt. J. Basic Appl. Sci. 4 (1), 74–79. https://doi.org/10.1016/j.ejbas.2016.11.002.

Ferrari, A.C., Meyer, J.C., Scardaci, V., Casiraghi, C., Lazzeri, M., Mauri, F., Geim, A.K., 2006. Raman spectrum of graphene and graphene layers. Phys. Rev. Lett. 97, (18). https://doi.org/10.1103/PhysRevLett.97.187401 187401.

Geim, A.K., Novoselov, K.S., 2007. The rise of graphene. Nat. Mater. 6 (3), 183–191. https://doi.org/10.1038/nmat1849.

Guerrero-Contreras, J., Caballero-Briones, F., 2015. Graphene oxide powders with different oxidation degree, prepared by synthesis variations of the Hummers method. Mater. Chem. Phys. 153, 209–220. https://doi.org/10.1016/j.matchemphys.2015.01.005.

He, J., Fang, L., 2016. Controllable synthesis of reduced graphene oxide. Curr. Appl Phys. 16 (9), 1152–1158. https://doi.org/10.1016/j.cap.2016.06.011.

Hummers, W.S., Offeman, R.E., 1958. Preparation of graphitic oxide 1339–1339 J. Am. Chem. Soc. 80 (6). https://doi.org/10.1021/ja01539a017.

Jeong, H.K., Yang, C., Kim, B.S., Kim, K.-J., 2010. Valence band of graphite oxide. EPL (Europhysics Letters) 92 (3), 37005. https://doi.org/10.1209/0295-5075/92/37005.

Jung, I., Field, D.A., Clark, N.J., Zhu, Y., Yang, D., Piner, R.D., Ruoff, R.S., 2009. Reduction kinetics of graphene oxide determined by electrical transport measurements and temperature programmed desorption. J. Phys. Chem. C 113 (43), 18480–18486. https://doi.org/10.1021/jp904396j.

Krishnamoorthy, K., Veerapandian, M., Mohan, R., Kim, S.-J., 2012. Investigation of Raman and photoluminescence studies of reduced

graphene oxide sheets. Appl. Phys. A 106 (3), 501–506. https://doi.org/10.1007/s00339-011-6720-6.

Low, F.W., Chin Hock, G., Kashif, M., Samsudin, N.A., Chau, C.F., Indah Utami, A.R., Lai, C.W., 2020a. Influence of sputtering temperature of TiO2 deposited onto reduced graphene oxide nanosheet as efficient photoanodes in dye-sensitized solar cells. Molecules 25 (20), 4852.

Low, F.W., Chin Hock, G., Kashif, M., Samsudin, N.A., Chau, C.F., Indah Utami, A.R., Tiong, S.K., 2020b. Influence of sputtering temperature of TiO(2) deposited onto reduced graphene oxide nanosheet as efficient photoanodes in dye-sensitized solar cells. Molecules 25 (20). https://doi.org/10.3390/molecules25204852.

Low, F.W., Lai, C.W., Abd Hamid, S.B., 2015. Easy preparation of ultrathin reduced graphene oxide sheets at a high stirring speed. Ceram. Int. 41 (4), 5798–5806. https://doi.org/10.1016/j.ceramint.2015.01.008.

Low, F.W., Lai, C.W., Abd Hamid, S.B., 2017. Surface modification of reduced graphene oxide film by Ti ion implantation technique for high dye-sensitized solar cells performance. Ceram. Int. 43 (1), 625–633. https://doi.org/10.1016/j.ceramint.2016.09.205.

Manoj, B., Raj, A.M., Chirayil, G.T., 2017. Tunable direct band gap photoluminescent organic semiconducting nanoparticles from lignite. Sci. Rep. 7 (1), 1–9.

Marcano, D.C., Kosynkin, D.V., Berlin, J.M., Sinitskii, A., Sun, Z., Slesarev, A., Tour, J.M., 2010. Improved synthesis of graphene oxide. ACS Nano 4 (8), 4806–4814. https://doi.org/10.1021/nn1006368.

Marrani, A.G., Coico, A.C., Giacco, D., Zanoni, R., Motta, A., Schrebler, R., Dalchiele, E.A., 2019. Flexible interfaces between reduced graphene oxide and indium tin oxide/polyethylene terephthalate for advanced optoelectronic devices. ACS Appl. Nano Mater. 2 (9), 5963–5972. https://doi.org/10.1021/acsanm.9b01399.

Mei, Q., Zhang, K., Guan, G., Liu, B., Wang, S., Zhang, Z., 2010. Highly efficient photoluminescent graphene oxide with tunable surface properties. Chem. Commun. 46 (39), 7319–7321. https://doi.org/10.1039/C0CC02374D.

Murakami, K., Miyaji, J., Furuya, R., Adachi, M., Nagao, M., Neo, Y., Mimura, H., 2019. High-performance planar-type electron source based on a graphene-oxide-semiconductor structure. Appl. Phys. Lett. 114, (21). https://doi.org/10.1063/1.5091585 213501.

Muzyka, R., Kwoka, M., Smędowski, Ł., Díez, N., Gryglewicz, G., 2017. Oxidation of graphite by different modified Hummers methods. New Carbon Mater. 32 (1), 15–20. https://doi.org/10.1016/S1872-5805(17)60102-1.

Novoselov, K.S., Geim, A.K., Morozov, S.V., Jiang, D., Zhang, Y., Dubonos, S.V., Firsov, A.A., 2004. Electric field effect in atomically thin carbon films. Science 306 (5696), 666–669. https://doi.org/10.1126/science.1102896.

Panicker, N.J., Das, J., Sahu, P.P., 2020. Synthesis of highly oxidized graphene (HOG) by using HNO3 and KMnO4 as oxidizing agents. Mater. Today: Proc. https://doi.org/10.1016/j.matpr.2020.05.037.

Pargoletti, E., Hossain, U.H., Di Bernardo, I., Chen, H., Tran-Phu, T., Chiarello, G.L., Cappelletti, G., 2020. Engineering of SnO2-graphene oxide nanoheterojunctions for selective room-temperature chemical sensing and optoelectronic devices. ACS Appl. Mater. Interfaces 12 (35), 39549–39560. https://doi.org/10.1021/acsami.0c09178.

Pimenta, M.A., Dresselhaus, G., Dresselhaus, M.S., Cançado, L.G., Jorio, A., Saito, R., 2007. Studying disorder in graphite-based systems by Raman spectroscopy. PCCP 9 (11), 1276–1290. https://doi.org/10.1039/B613962K.

Qu, Y., He, F., Yu, C., Liang, X., Liang, D., Ma, L., Wu, J., 2018. Advances on graphene-based nanomaterials for biomedical applications. Mater. Sci. Eng., C 90, 764–780. https://doi.org/10.1016/j.msec.2018.05.018.

Shamaila, S., Sajjad, A.K.L., Iqbal, A., 2016. Modifications in development of graphene oxide synthetic routes. Chem. Eng. J. 294, 458–477. https://doi.org/10.1016/j.cej.2016.02.109.

Skákalová, V., Kotrusz, P., Jergel, M., Susi, T., Mittelberger, A., Vretenár, V., Hulman, M., 2018. Chemical oxidation of graphite: evolution of the structure and properties. J. Phys. Chem. C 122 (1), 929–935.

Soldano, C., Mahmood, A., Dujardin, E., 2010. Production, properties and potential of graphene. Carbon 48 (8), 2127–2150. https://doi.org/10.1016/j.carbon.2010.01.058.

Thota, A., Wang, Q., Liu, P., Jian, Z., 2021. Highly electrochemical active composites based on capacitive graphene/aniline oligomer hybrid for high-performance sustainable energy storage devices. Electrochim. Acta 368,. https://doi.org/10.1016/j.electacta.2020.137587 137587.

Veerapandian, M., Lee, M.-H., Krishnamoorthy, K., Yun, K., 2012. Synthesis, characterization and electrochemical properties of functionalized graphene oxide. Carbon 50 (11), 4228–4238. https://doi.org/10.1016/j.carbon.2012.05.004.

Venugopal, G., Jung, M.-H., Suemitsu, M., Kim, S.-J., 2011. Fabrication of nanoscale three-dimensional graphite stacked-junctions by focused-ion-beam and observation of anomalous transport characteristics. Carbon 49 (8), 2766–2772. https://doi.org/10.1016/j.carbon.2011.03.003.

Venugopal, G., Krishnamoorthy, K., Mohan, R., Kim, S.-J., 2012. An investigation of the electrical transport properties of graphene-oxide thin films. Mater. Chem. Phys. 132 (1), 29–33. https://doi.org/10.1016/j.matchemphys.2011.10.040.

Wang, B., Kanhere, P.D., Chen, Z., Nisar, J., Pathak, B., Ahuja, R., 2013. Anion-doped NaTaO3 for visible light photocatalysis. J. Phys. Chem. C 117 (44), 22518–22524. https://doi.org/10.1021/jp407025r.

Wang, H., Zhang, C., Liu, Z., Wang, L., Han, P., Xu, H., Cui, G., 2011. Nitrogen-doped graphene nanosheets with excellent lithium storage properties. J. Mater. Chem. 21 (14), 5430–5434. https://doi.org/10.1039/C1JM00049G.

Yahia, I., Mohammed, M., 2018. Facile synthesis of graphene oxide/PVA nanocomposites for laser optical limiting: band gap analysis and dielectric constants. J. Mater. Sci.: Mater. Electron. 29 (10), 8555–8563.

Yang, Y., Chen, S., Li, W., Li, P., Ma, J., Li, B., Liu, Y., 2020. Reduced graphene oxide conformally wrapped silver nanowire networks for flexible transparent heating and electromagnetic interference shielding. ACS Nano 14 (7), 8754–8765. https://doi.org/10.1021/acsnano.0c03337.

Zhang, R., Palumbo, A., Kim, J.C., Ding, J., Yang, E.H., 2019. Flexible graphene-, graphene-oxide-, and carbon-nanotube-based supercapacitors and batteries. Ann. Phys. 531 (10), 1800507. https://doi.org/10.1002/andp.201800507.

Zhou, Y., Maleski, K., Anasori, B., Thostenson, J.O., Pang, Y., Feng, Y., Cao, C., 2020. Ti3C2Tx MXene-reduced graphene oxide composite electrodes for stretchable supercapacitors. ACS Nano 14 (3), 3576–3586. https://doi.org/10.1021/acsnano.9b10066.